

## Update on Glueballs

---

**Colin Morningstar**<sup>a,\*</sup>

<sup>a</sup>*Department of Physics, Carnegie Mellon University, Pittsburgh, Pennsylvania 15213, USA*

*E-mail:* [cmorning@andrew.cmu.edu](mailto:cmorning@andrew.cmu.edu)

The recent BESIII announcement of a pseudoscalar glueball candidate makes an update on glueballs from lattice QCD timely. A brief review of how glueballs are studied in lattice QCD is given, and the reasons that glueballs are difficult to study both in lattice QCD with dynamical quarks and in experiments are outlined. Recent glueball studies in lattice QCD are then presented, and an exploratory investigation of the scalar glueball using glueball, meson, and meson-meson operators is summarized, suggesting that no scalar state below 2 GeV or so can be considered to be predominantly a glueball state.

*The 41st International Symposium on Lattice Field Theory (LATTICE2024)*  
*28 July - 3 August 2024*  
*Liverpool, UK*

---

\*Speaker

## 1. Introduction

An update on glueballs from lattice QCD is timely now due to a first-time determination by BESIII of the  $0^{-+}$  quantum numbers of the  $X(2370)$  resonance[1]. This resonance, previously found in  $J/\psi \rightarrow \gamma\pi^+\pi^-\eta'$  and reported in Ref. [2], occurs in a gluon rich environment (see Fig. 1) and its mass is consistent with the lightest  $0^{-+}$  glueball from pure-gauge lattice QCD[3–7] (see Fig. 2), leading some to speculate that it might be a glueball. A partial wave analysis (PWA) of  $J/\psi \rightarrow \gamma K_S^0 K_S^0 \eta'$  gives

$$m = 2395 \pm 11(\text{stat})_{-94}^{+26}(\text{syst}) \text{ MeV}/c^2, \quad (1)$$

$$\Gamma = 188_{-17}^{+18}(\text{stat})_{-33}^{+124}(\text{syst}) \text{ MeV}. \quad (2)$$

The optimal PWA fit (see Fig. 2) contains the  $X(1835)$ ,  $X(2370)$ ,  $\eta_c$  and a broad  $0^{-+}$   $X(2800)$  Breit-Wigner with decays through  $f_0(980)\eta'$  to  $(K_S^0 K_S^0)_S \eta'$  and  $(K_S^0 K_S^0)_D \eta'$  with nonresonant components, producing a statistical significance of the  $X(2370)$  of  $> 11.7\sigma$ .

Identifying a glueball in experiments is notoriously difficult. First, there are no reliable estimates of their masses from theory to help guide experimental searches. To date, lattice QCD has only provided reliable glueball mass determinations in the pure gauge theory without dynamical quarks. Second, one expects flavor symmetric decays, but differing quark masses can lead to differing phase spaces which could affect branching ratios. There are no rigorous predictions from theory on decay patterns and their branching ratios. Glueball decays could be similar to that of charmonium states, and observed resonances could be admixtures having both glueball and quark-antiquark components. Early glueball candidates were the light scalar candidates  $f_0(1370)$ ,  $f_0(1500)$ ,  $f_0(1710)$  from MarkII in the 1980s and Crystal Barrel in the 1990s. The narrow  $\xi(2230)$  tensor glueball candidate from MarkIII in the 1980s and BESI in the 1990s possessed good flavor-symmetric decay properties, but its existence was not confirmed later by BESII nor BESIII with much higher statistics. An odderon (odd  $C$ -parity) from D0 and TOTEM[8] has also been suggested as a glueball candidate. Given the above considerations, an identification of the latest pseudoscalar candidate from BESIII as a glueball cannot be considered definitive.

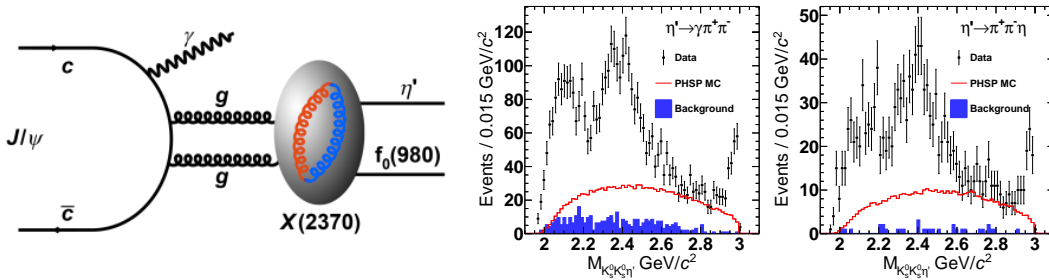


**Figure 1:** Left: a typical process in BESIII which can produce the  $X(2370)$ . Right: the  $K_S^0 K_S^0 \eta'$  invariant mass distributions with the requirement  $M_{K_S^0 K_S^0} < 1.1 \text{ GeV}/c^2$  for  $\eta' \rightarrow \gamma\pi^+\pi^-$  and  $\eta' \rightarrow \pi^+\pi^-\eta$  channels. Data are indicated by the dots with error bars, and the shaded histograms are the non- $\eta'$  backgrounds. The solid red lines are phase space Monte Carlo events with arbitrary normalization. Plots are taken from Ref. [1].

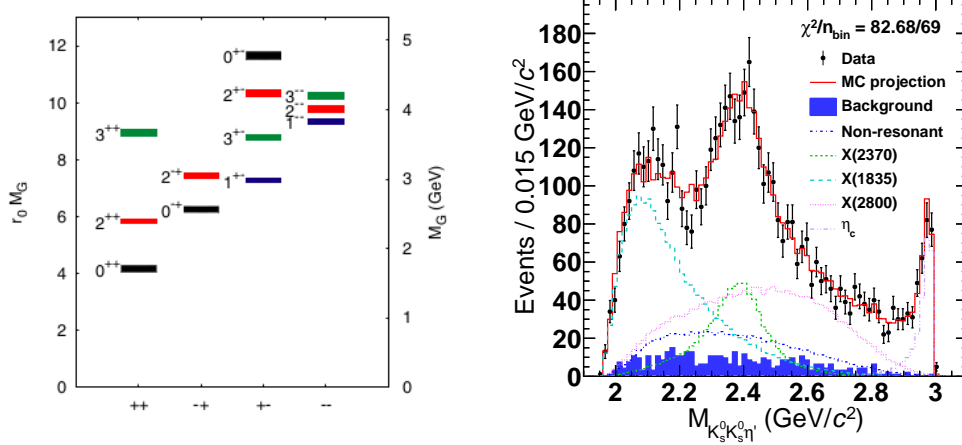


**Figure 2:** Left: the mass spectrum of glueballs in the pure gauge Yang-Mills theory from Ref. [5]. The masses are given both in terms of  $r_0$  ( $r_0^{-1} = 410$  MeV) and in GeV. The height of each colored box indicates the statistical uncertainty of the mass. Right: a comparison between data and PWA fit projections from Ref. [1] showing the invariant mass distributions of  $K_S^0 K_S^0 \eta'$ . Data show as dots with error bars, and the solid red histograms are the PWA total projections. The shaded histograms are the non- $\eta'$  backgrounds. Contributions from the  $X(2370)$ ,  $X(1835)$ ,  $X(2800)$ ,  $\eta_c$ , and non-resonant processes are shown by the short dashed green, long dashed cyan, dotted magenta, dash-dot-dotted violet, and dash-dotted blue lines, respectively.

The pure-gauge glueball spectrum has a long history in lattice QCD, with calculations dating back to early days of lattice QCD in the 1970s. Given their heavy masses (the lightest is around 1.6 GeV), the temporal correlators used to extract their masses fall off very rapidly in imaginary time with statistical uncertainties that do not diminish significantly with time, leading to a very quickly degrading signal-to-noise in Markov-chain Monte Carlo computations as the temporal separation of the source and sink operators increases. Significant progress in calculating the spectrum of glueballs was made in the 1980s and 1990s by M. Teper, C. Michael, D. Weingarten, among others. The introduction of anisotropic lattices in the late 1990s allowed much better temporal resolution of the correlators, significantly improving glueball energy determinations. Today, the mass spectrum of glueballs in the pure-gauge Yang-Mills theory is well known (see Fig. 2). Their mass ratios are well determined, but obtaining their masses in MeV, for example, is less straightforward due to scale setting ambiguities. The pure-gauge theory is not physical (quark loops cannot be suppressed in nature), so setting any quantity computed in the pure-gauge theory by using the value of the analogous observable obtained in experiment is problematic. The string tension from the static quark-antiquark potential or some variant of it is generally used to set the scale, leading to the lightest glueball having a mass around 1600 – 1700 MeV. The Clay Mathematics Institute is offering a \$1 million bounty[9] for a mathematical proof of the existence of the mass gap of the lightest glueball, which has the quantum numbers of a scalar particle. This Yang-Mills mass gap is one of its Millenium Prize problems.

In lattice QCD, finite-volume stationary-state energies are extracted from a matrix of temporal correlation functions,  $C_{ij}(t) = \langle 0 | O_i(t) \bar{O}_j(0) | 0 \rangle$ , where the set of operators  $\bar{O}_i(t)$  creates the states of interest at imaginary time  $t$ . In the scalar channel, a vacuum-expectation value subtraction

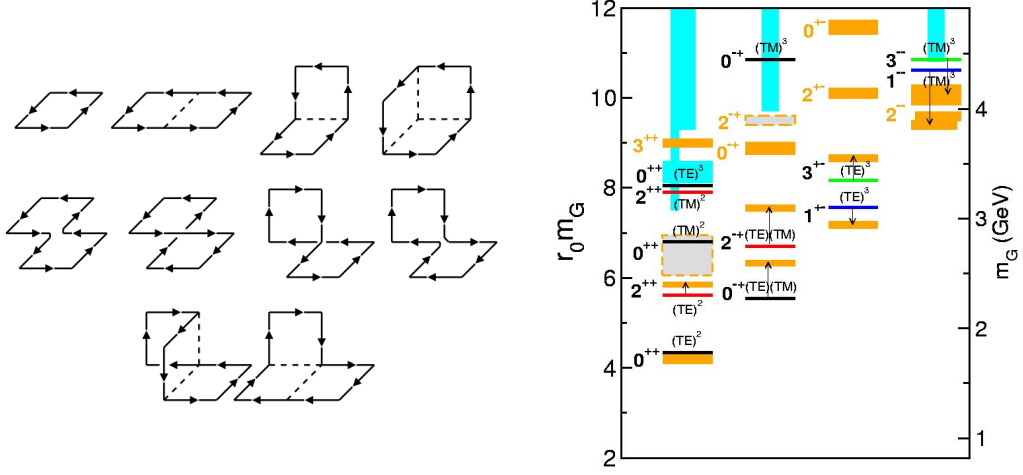


**Figure 3:** Left: the various typical Wilson loop shapes used in making glueball operators. Each link represents a smeared path which is one or more lattice spacings in length. Right: comparison of the glueball spectrum from the MIT bag model (with revised parameter values) with that from lattice QCD (shown as orange boxes).

is useful. Because of the finite spatial volume and the usual imposition of periodic boundary conditions, the energies of the stationary states are discrete. Neglecting temporal wrap-around effects, these correlation matrix elements have spectral representations of the form

$$C_{ij}(t) = \sum_n Z_i^{(n)} Z_j^{(n)*} e^{-E_n t}, \quad Z_j^{(n)} = \langle 0 | O_j | n \rangle.$$

It is not practical to do fits using the above form due to the large number of unknown parameters that must be determined. To extract the finite-volume energies  $E_n$  and operator overlap factors  $Z_j^{(n)}$ , we define a new correlation matrix  $\tilde{C}(t)$  using a single pivot

$$\tilde{C}(t) = U_D^\dagger C(\tau_0)^{-1/2} C(t) C(\tau_0)^{-1/2} U_D,$$

where the columns of  $U_D$  are the eigenvectors of  $C(\tau_0)^{-1/2} C(\tau_D) C(\tau_0)^{-1/2}$ , with  $\tau_D > \tau_0$ . We choose  $\tau_0$  and  $\tau_D$  large enough so that the matrix  $\tilde{C}(t)$  stays diagonal, within statistical errors, for  $t > \tau_D$ . Then we can use single- or two-exponential fits to  $\tilde{C}_{\alpha\alpha}(t)$  to obtain the energies  $E_\alpha$  and overlaps  $Z_j^{(n)}$ .

Due to the unfavorable signal-to-noise of correlators involving glueball operators, it is imperative to use very good operators to ensure reliable energy extractions at time separations as small as possible. Fortunately, much work has been done in designing such operators. First, a variety of spatial link smearings are performed, such as Teper fuzzing[10] and stout-link smearing[11]. In particular, Teper fuzzing creates paths which are one or more lattice links long, allowing spatially large operators to be efficiently evaluated. Glueball operators are then formed from gauge-invariant loops of the smeared link variables, such as those shown in Fig. 3. Multiple sizes of loops with different shapes are constructed to build up the necessary radial and orbital structures.

The glueball spectrum can be qualitatively understood in terms of interpolating operators of minimal dimension, as first outlined long ago in Ref. [12] and listed in Table 1. Of the lightest six

**Table 1:** Quantum numbers associated with the glueball operators of minimal dimension, taken from Ref. [12]

Dimension	Operators	Quantum numbers
4	$\text{Tr}F_{\mu\nu}F_{\alpha\beta}$	$0^{++}, 0^{-+}, 2^{++}, 2^{-+}$
5	$\text{Tr}F_{\mu\nu}D_{\rho}F_{\alpha\beta}$	$1^{++}, 3^{++}$
6	$\text{Tr}F_{\mu\nu}F_{\rho\omega}F_{\alpha\beta}$	$0^{\pm\pm}, 1^{\pm\pm}, 2^{\pm\pm}, 3^{\pm-}$
6	$\text{Tr}F_{\mu\nu}\{D_{\rho}, D_{\omega}\}F_{\alpha\beta}$	$1^{-+}, 3^{-+}, 4^{\pm+}$

glueball states from lattice QCD, four have the  $J^{PC}$  of the dimension-four operators, and the absence of low-lying  $0^{\pm-}$ ,  $1^{-+}$  glueballs is explained. The spectrum also agrees qualitatively with the MIT bag model, as shown in Fig. 3. In this early model, constituent gluons are transverse chromoelectric (TE) or transverse chromomagnetic (TM) modes in a spherical cavity, and the spectrum is obtained from Hartree modes with residual perturbative interactions and a center-of-mass correction. The results in Fig. 3 come from Ref. [13] with parameter modifications suggested in Ref. [14]: strong coupling  $\alpha_s : 1.0 \rightarrow 0.5$  and bag parameter  $B^{1/4} : 230 \text{ MeV} \rightarrow 280 \text{ MeV}$ . The flux-tube model of glueballs in Ref. [15] yields a mass spectrum in striking disagreement with that from lattice QCD.

Studying glueballs in lattice QCD with dynamical quarks is very challenging. To extract the energies of the heavy glueball states, the energies of all levels lying below the glueballs of interest must also be extracted, and there are many two-meson, three-meson, and four-meson levels expected. Multi-meson correlators typically require costly timeslice-to-timeslice propagators. Glueballs are expected to be unstable resonance states whose masses and widths must be deduced from fits of scattering  $K$ -matrix parametrizations to the finite-volume spectra via a Lüscher quantization condition. Carrying out such fits can be a daunting task. As previously mentioned, correlators involving glueballs are statistically noisy, so high statistics are required which is very difficult with dynamical quarks. Large vacuum expectation values must also be subtracted in the scalar sector, exacerbating the difficulties.

## 2. Some recent glueball studies

In the remainder of this talk, I highlight some recent glueball studies in lattice QCD.

### 2.1 Glueballs with $N_f = 4$ light quarks

A study of glueballs with  $N_f = 4$  light quarks has recently been presented in Ref. [16] with the goal of examining the effect of quark loops on the glueball spectrum. Several ensembles were used with  $m_{\pi} \approx 250 \text{ MeV}$ . The energies obtained are compared to the pure gauge theory in Fig. 4. In this figure, one sees that the scalar results are lowered towards the  $2\pi$  threshold, and the tensor and pseudoscalar masses are only slightly affected. This work is exploratory since only glueball operators were used. No meson-meson operators were incorporated into the study. The topological charge is evaluated, and the string tension is found to be suppressed by the inclusion of four light dynamical quarks by 50-70%, compared to the pure gauge theory.

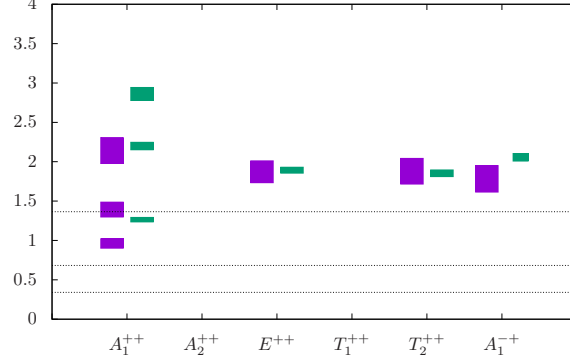


**Figure 4:** The spectrum of glueballs for the representations  $A^{++}$ ,  $E^{++}$ ,  $T_2^{++}$ ,  $A_1^{-+}$  from Ref. [16]. The vertical scale is mass times  $\sqrt{t_0}$ , where  $t_0$  is the usual gradient flow parameter[17]. Results from  $N_f = 4$  QCD for a particular ensemble are shown in purple, while the states in SU(3) pure gauge are shown in green. The dashed lines correspond to 1, 2 and 4 times the pion mass from bottom to top, respectively.

## 2.2 Radiative decay of the scalar glueball

The radiative decay of the scalar glueball was studied in the quenched approximation in Ref. [18] using three gauge ensembles with lattice spacings  $a_s \sim 0.11, 0.14, 0.22$  fm and extrapolating to the continuum limit. The EM transition matrix element  $\langle S | J_{\text{em}}^\mu | V \rangle$  was evaluated and a multipole expansion used to obtain two form factors  $E_1(Q^2)$  and  $C_1(Q^2)$ . Decay widths are obtained from  $E_1(0)$  using  $Q^2 \rightarrow 0$ ,  $a \rightarrow 0$  extrapolations. The continuum limit extrapolations for  $E_1(0)$  for the  $J/\psi \rightarrow \gamma G$  and  $J/\psi \rightarrow \gamma \phi$  processes are shown in Fig. 5. This work finds  $\Gamma(J/\psi \rightarrow \gamma G) = 0.578(86)$  keV with  $\text{Br}(J/\psi \rightarrow \gamma G) = 6.2(9) \times 10^{-3}$  and  $\Gamma(G \rightarrow \gamma \phi) = 0.074(47)$  keV, concluding that  $J\psi \rightarrow \gamma G \rightarrow \gamma\gamma\phi$  is not detectable by BESIII.

## 2.3 Error reduction algorithm

In Ref. [19], a new multi-level sampling procedure was proposed for error reduction of glueball correlators in the pure SU(3) gauge theory. Comparisons of some glueball masses obtained using

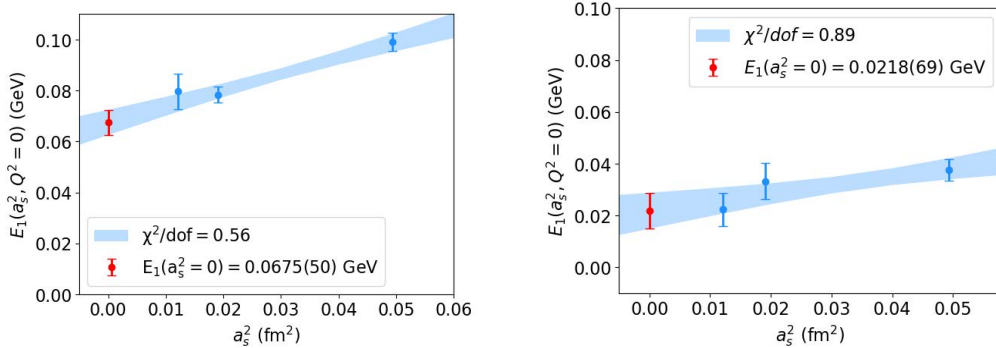


**Figure 5:** Linear continuum limit extrapolations of the  $E_1$  form factors for the  $J/\psi \rightarrow \gamma G$  process (left) and  $J/\psi \rightarrow \gamma \phi$  (right) using three different lattice spacings from Ref. [18].

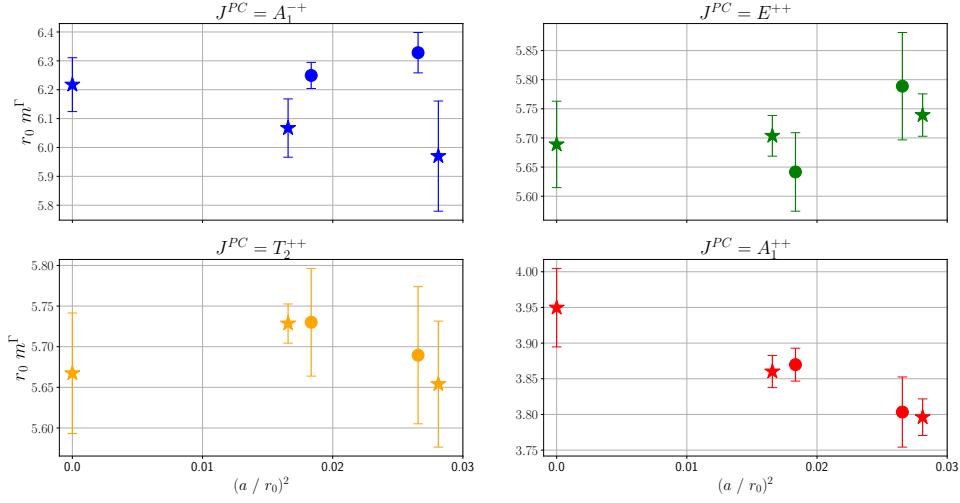


**Figure 6:** Comparison between Wilson-action glueball masses obtained in Ref. [19] at  $\beta = 6.2, 6.08$  using a new multi-level error reduction algorithm (circles) and state-of-the-art results (stars) at  $\beta = 6.0625, 6.235$  and in the continuum limit from a recent study[20] using the traditional Monte Carlo algorithm.

this new method with masses obtained using the traditional procedure[20] are shown in Fig. 6 for the Wilson action. Although no significant reduction in the glueball mass errors were observed, significant error reduction in large- $t$  correlators were found, which improves confidence in plateau estimates.

## 2.4 Glueball- $\eta$ mixing

The mixing of the  $0^{-+}$  glueball and the pseudoscalar  $\eta$  meson was studied in Ref. [21], with results shown in Fig. 7. Results were obtained on a  $16^3 \times 128$  anisotropic  $N_f = 2$  lattice with  $m_\pi \approx 350$  MeV. The distillation method[22] was utilized. The pseudoscalar glueball operator was constructed using a variationally optimized superposition of a variety of smeared gauge-invariant

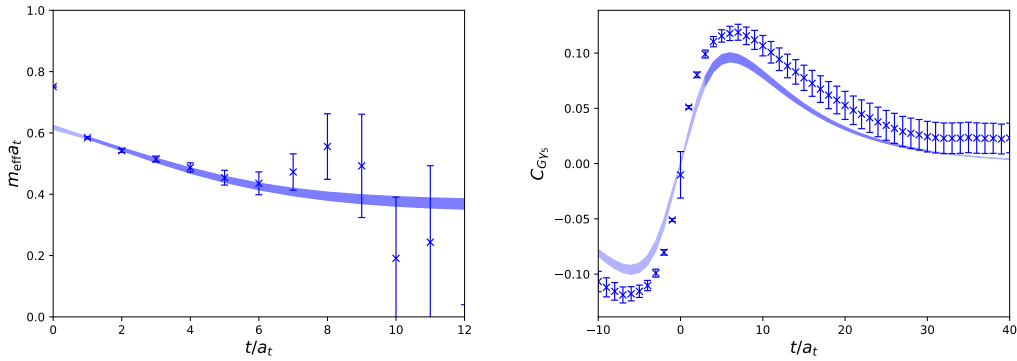


**Figure 7:** (Left) Effective mass for the  $0^{-+}$  glueball correlator from Ref. [21]. The shaded band shows the result from a forward and backward two-exponential fit. (Right) The glueball- $\eta$  cross correlator (shifted horizontally). The blue band shows the result from a fit to the temporal derivative of the correlator using forward-backward exponentials with four masses.

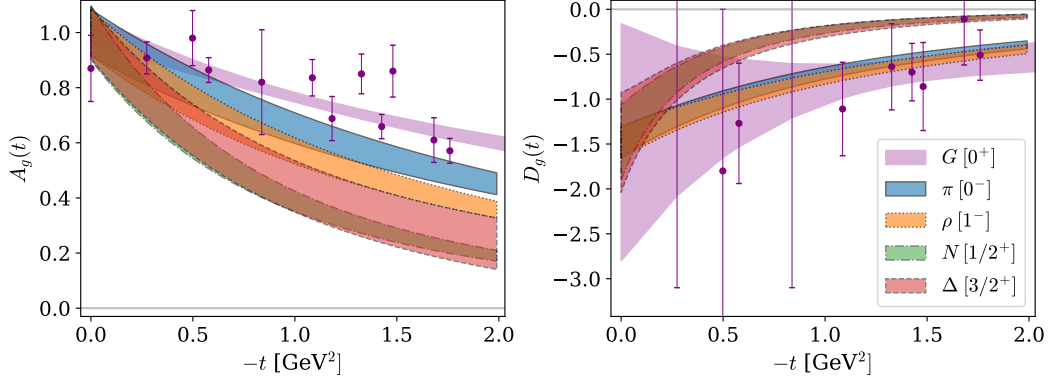


**Figure 8:** Comparison between the scalar glueball GFFs in Yang-Mills theory obtained in Ref. [23] and the gluon GFFs from Ref. [24] of the pion,  $\rho$  meson, nucleon, and  $\Delta$  baryon, obtained with an  $N_f = 2 + 1$  QCD ensemble with  $m_\pi = 450$  MeV. As usual,  $t = (p' - p)^2$ , where  $p$  and  $p'$  are the four-momenta of the incoming and outgoing states.

loops, as usual. The  $\eta$  operator used was a local  $\bar{q}\gamma_5 q$  operator using smeared quark fields, although  $\bar{q}\gamma_4\gamma_5 q$  was also considered. The diagonal and cross correlators were computed, and a very small  $3.5^\circ$  mixing angle was obtained from the glueball- $\eta$  cross correlator.

## 2.5 Gravitational form factors of glueballs

In Ref. [23], a first step towards probing the structure of glueballs using gravitational form factors (GFF) was presented at this conference. The GFFs are obtained from the energy-momentum tensor matrix elements in SU(3) pure gauge theory. The matrix element of  $T_{\mu\nu}$  in the scalar glueball state can be expressed in terms of two form factors  $A(t)$  and  $D(t)$ , with  $t = (p' - p)^2$  and where  $p$  and  $p'$  are the four-momenta of the incoming and outgoing states. Preliminary results in pure gauge theory on a  $24^3 \times 48$  lattice with spacing  $a = 0.1$  fm were presented and are shown in Fig. 8. The glueball GFFs in this figure are compared to gluon GFFs from Ref. [24] of the pion,  $\rho$  meson, nucleon, and  $\Delta$  baryon, obtained with an  $N_f = 2+1$  QCD ensemble with  $m_\pi = 450$  MeV.

## 2.6 Scalar glueball scattering

First steps towards computing glueball-glueball scattering in lattice QCD were presented in Ref. [25]. In this study, finite-volume energies in Yang-Mills involving both single and two scalar glueball operators were computed. An anisotropic lattice was used, a multi-level algorithm was employed to reduce correlator errors, and scale setting was done using the gradient flow parameter  $t_0$  [17]. The vol-

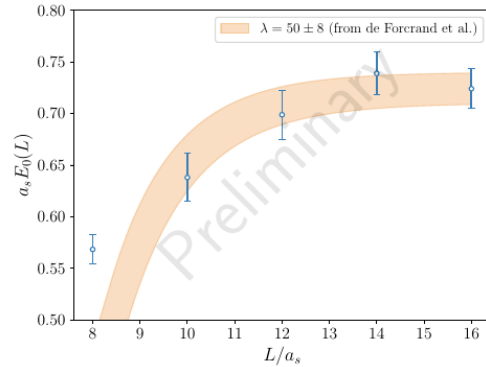


**Figure 9:** The  $A_1^{++}$  energy in pure Yang-Mills in finite volume  $L^3$  from Ref. [25] against  $L$ . The trilinear coupling  $\lambda$  was then extracted by a fit to the Lüscher relation.



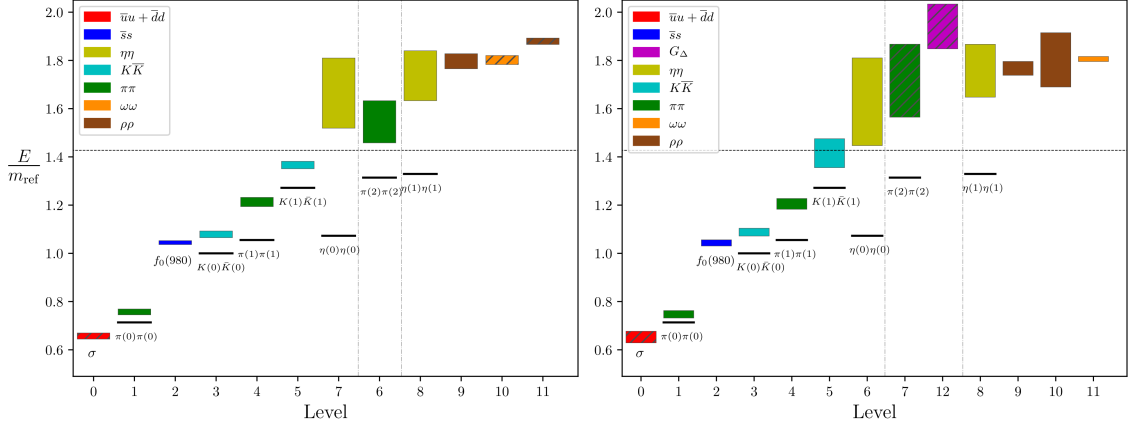


**Figure 10:** Finite-volume stationary state energies in the  $I = 0, S = 0, A_{1g}^+$  channel extracted using a  $12 \times 12$  correlation matrix, *excluding* the scalar glueball operator on the left, and using a  $13 \times 13$  correlation matrix *including* the scalar glueball operator on the right.  $1\sigma$  uncertainties are denoted by the box heights. If a level is created predominantly by a single operator, the level is colored to indicate the flavor content of that operator. If a level is created predominantly by more than one operator, a hatched box is used to denote the presence of operator overlaps within 75% of the maximum, indicating significant mixing. Level numbers indicate order in terms of increasing mean energy, but the levels have been rearranged horizontally to highlight the area of interest involving the glueball operator. Short black lines indicate the non-interacting two-hadron levels, and the dashed horizontal black line indicates the  $4\pi$  threshold, and  $m_{\text{ref}} = 2m_K$ .

ume dependence of the  $A_1^{++}$  energy was evaluated and is shown in Fig. 9. The Lüscher relation was then utilized to get the trilinear coupling  $\lambda$  from these energies.

## 2.7 Scalar glueball in $N_f = 2 + 1$ QCD

The scalar glueball in the presence of dynamical quarks has been studied previously in Refs. [26, 27]. Although this work was reported back in 2019, its incorporation of glueball, single quark-antiquark meson, and meson-meson operators makes it still of interest at present. This work was done on a small  $24^3 \times 128$  anisotropic lattice with  $m_\pi \sim 390$  MeV using the stochastic LapH method[28]. The main goal in this study was to discover if any finite-volume states below  $2m_{\text{ref}}$  in the vacuum sector are *missed* when no glueball operators are included, where  $m_{\text{ref}} = 2m_K$ . The results are summarized in Fig. 10. In the left plot of this figure, the finite-volume spectrum determined using a basis of interpolating operators *excluding* the scalar glueball operator is shown. A two-hadron (meson-meson) operator for each expected non-interacting level is included, and additional operators with various flavor, spin, and orbital structure are added until no new finite-volume levels were found below  $\sim 2m_{\text{ref}}$ . Single-hadron  $\bar{q}q$  operators are chosen in a similar way, including one of each isoscalar flavor structure:  $(\bar{u}u + \bar{d}d, \bar{s}s)$  with various spatial displacements until no new states are seen in the energy region of interest. In the end, two  $\bar{q}q$  operators and ten two-meson operators were included to produce a  $12 \times 12$  correlation matrix. In the right plot of Fig. 10, the spectrum obtained using a  $13 \times 13$  correlation matrix including the twelve operators discussed above plus a scalar glueball operator is shown. The low-lying spectrum is essentially unchanged. An additional level, shown as the purple hatched box, appears very high in the spectrum.

Overlap factors associated with each operator are used to identify the energy levels in Fig. 10. These results indicate that no finite-volume energy eigenstate below  $\sim 1.9m_{\text{ref}}$  can be identified as being predominantly created by a scalar glueball operator. As the single new energy occurs above the region where our operator set is designed to create states, no reliable inferences can be drawn about this state.

While these finite-volume results are insufficient to make any definitive statements regarding the infinite-volume resonances in this channel, we can make some qualitative comparisons to experiment. In finding only two  $\bar{q}q$  dominated states below  $2m_{\text{ref}}$ , we have observed no clearly identifiable counterpart finite-volume  $\bar{q}q$  states to the  $f_0(1370)$ ,  $f_0(1500)$ , or  $f_0(1710)$  resonances in this region. This suggests that these resonances are molecular in nature rather than conventional  $\bar{q}q$  or pure glueball states.

### 3. Conclusion

In this talk, some recent glueball studies were highlighted. Glueballs are very challenging to study in lattice QCD with dynamical quarks, but progress is being made. One recent study suggests that no scalar state below 2 GeV is predominantly a glueball state. Due to a first-time determination by BESIII of the  $0^{-+}$  quantum numbers of the  $X(2370)$  resonance, the pseudoscalar glueball is a new focus of attention. Identifying glueballs in experiments is very challenging too. Glueballs have a long history in lattice QCD, and their interesting features and the challenges of studying them ensure they will have a long future as well. I acknowledge support from the U.S. NSF under award PHY-2209167.

### References

- [1] BESIII collaboration, *Determination of Spin-Parity Quantum Numbers of  $X(2370)$  as  $0^{-+}$  from  $J/\psi \rightarrow \gamma K_S^0 K_S^0 \eta'$* , *Phys. Rev. Lett.* **132** (2024) 181901.
- [2] BESIII collaboration, *Confirmation of the  $X(1835)$  and Observation of the Resonances  $X(2120)$  and  $X(2370)$  in  $J/\psi \rightarrow \gamma \pi^+ \pi^- \eta'$* , *Phys. Rev. Lett.* **106** (2011) 072002.
- [3] G. Bali, K. Schilling, A. Hulsebos, A. Irving, C. Michael and P. Stephenson, *A comprehensive lattice study of  $SU(3)$  glueballs*, *Physics Letters B* **309** (1993) 378.
- [4] C.J. Morningstar and M. Peardon, *Glueball spectrum from an anisotropic lattice study*, *Phys. Rev. D* **60** (1999) 034509.
- [5] Y. Chen, A. Alexandru, S.J. Dong, T. Draper, I. Horváth, F.X. Lee et al., *Glueball spectrum and matrix elements on anisotropic lattices*, *Phys. Rev. D* **73** (2006) 014516.
- [6] E. Gregory, A. Irving, B. Lucini, C. McNeile, A. Rago, C. Richards et al., *Towards the glueball spectrum from unquenched lattice QCD*, *JHEP* **10** (2012) 170.
- [7] L.-C. Gui, J.-M. Dong, Y. Chen and Y.-B. Yang, *Study of the pseudoscalar glueball in  $J/\psi$  radiative decays*, *Phys. Rev. D* **100** (2019) 054511.

- [8] D0 AND TOTEM collaboration, *Odderon Exchange from Elastic Scattering Differences between  $pp$  and  $p\bar{p}$  Data at 1.96 TeV and from  $pp$  Forward Scattering Measurements*, *Phys. Rev. Lett.* **127** (2021) 062003.
- [9] “Clay Mathematics Institute Millenium Prize Problems: Yang-Mills and the Mass Gap.” <https://www.claymath.org/millennium/yang-mills-the-maths-gap>.
- [10] M. Teper, *An improved method for lattice glueball calculations*, *Physics Letters B* **183** (1987) 345.
- [11] C. Morningstar and M.J. Peardon, *Analytic smearing of  $SU(3)$  link variables in lattice QCD*, *Phys. Rev. D* **69** (2004) 054501.
- [12] R. Jaffe, K. Johnson and Z. Ryzak, *Qualitative features of the glueball spectrum*, *Annals of Physics* **168** (1986) 344.
- [13] C.E. Carlson, T.H. Hansson and C. Peterson, *Meson, baryon, and glueball masses in the MIT bag model*, *Phys. Rev. D* **27** (1983) 1556.
- [14] J. Kuti. private communication.
- [15] N. Isgur and J. Paton, *Flux-tube model for hadrons in QCD*, *Phys. Rev. D* **31** (1985) 2910.
- [16] A. Athenodorou, J. Finkenrath, A. Lantos and M. Teper, *Glueball Spectrum with four light dynamical fermions*, [2308.10054](https://arxiv.org/abs/2308.10054).
- [17] M. Lüscher, *Properties and uses of the Wilson flow in lattice QCD*, *JHEP* **08** (2010) 071 [Erratum: *JHEP* **03** (2014) 092] [[1006.4518](https://arxiv.org/abs/1006.4518)].
- [18] J. Zou, L.-C. Gui, Y. Chen, W. Qin, J. Liang, X. Jiang et al., *The radiative decay of scalar glueball from lattice QCD*, *Sci. China Phys. Mech. Astron.* **67** (2024) 111012 [[2404.01564](https://arxiv.org/abs/2404.01564)].
- [19] L. Barca, S. Schaefer, F. Knechtli, J.A. Urrea-Niño, S. Martins and M. Peardon, *Exponential error reduction for glueball calculations using a two-level algorithm in pure gauge theory*, *Phys. Rev. D* **110** (2024) 054515 [[2406.12656](https://arxiv.org/abs/2406.12656)].
- [20] A. Athenodorou and M. Teper, *The glueball spectrum of  $SU(3)$  gauge theory in  $3 + 1$  dimensions*, *JHEP* **11** (2020) 172 [[2007.06422](https://arxiv.org/abs/2007.06422)].
- [21] X. Jiang, W. Sun, F. Chen, Y. Chen, M. Gong, Z. Liu et al.,  *$\eta$ -glueball mixing from  $N_f = 2$  lattice QCD*, *Phys. Rev. D* **107** (2023) 094510 [[2205.12541](https://arxiv.org/abs/2205.12541)].
- [22] HADRON SPECTRUM collaboration, *A Novel quark-field creation operator construction for hadronic physics in lattice QCD*, *Phys. Rev. D* **80** (2009) 054506 [[0905.2160](https://arxiv.org/abs/0905.2160)].
- [23] R. Abbott, D.C. Hackett, D.A. Pefkou, F. Romero-López and P. Shanahan, *Gravitational form factors of glueballs in Yang-Mills theory*, *PoS LATTICE2024* (2025) 459 [[2410.02706](https://arxiv.org/abs/2410.02706)].
- [24] D.A. Pefkou, D.C. Hackett and P.E. Shanahan, *Gluon gravitational structure of hadrons of different spin*, *Phys. Rev. D* **105** (2022) 054509 [[2107.10368](https://arxiv.org/abs/2107.10368)].

- 
- [25] M. Hansen, M. Bruno and A. Rago, *Towards glueball scattering in lattice Yang-Mills theory*, *PoS LATTICE2024* (2025) 127.
- [26] R. Brett, J. Bulava, D. Darvish, J. Fallica, A. Hanlon, B. Hörz et al., *Spectroscopy From The Lattice: The Scalar Glueball*, *AIP Conf. Proc.* **2249** (2020) 030032 [[1909.07306](#)].
- [27] R. Brett, *The Scalar Glueball and  $K\pi$  Scattering from Lattice QCD*, Ph.D. thesis, Carnegie Mellon University, 2019.
- [28] C. Morningstar, J. Bulava, J. Foley, K.J. Juge, D. Lenkner, M. Peardon et al., *Improved stochastic estimation of quark propagation with Laplacian Heaviside smearing in lattice QCD*, *Phys. Rev. D* **83** (2011) 114505 [[1104.3870](#)].